# Quench Protection Study of the Eurocircol 16 T cosθ Dipole for the Future Circular Collider (FCC)

Vittorio Marinozzi, Giovanni Bellomo, Barbara Caiffi, Pasquale Fabbricatore, Stefania Farinon, Tiina Salmi, Massimo Sorbi, Antti Stenvall, and Giovanni Volpini

***Abstract*—After LHC will be turned off, a new, more energetic machine will be needed in order to explore unknown regions of the high-energy physics. For this reason, the project Future Circular Collider (FCC) has started, with the goal of developing a 100 km circumference collider of 50 TeV proton beams. The Eurocircol collaboration is part of the FCC study under the European Community leadership, and it aims to develop a conceptual design of FCC within 2019. One of the main targets is to design a bending dipole able to reach 16 T operation magnetic field, in order to accomplish the size and energy constraints. Such a magnetic field can be reached using Nb3Sn conductors at their highest performance. One option under exploration is the Cosθ dipole, by INFN of Milano and Genova. One of the aspects to be taken into consideration is the amount of conductor needed, because of the relatively high cost of superconducting cables involving Nb3Sn. The amount of superconductor in the cross-section conductor area is a discriminant element for the choice of the magnet lay-out. At the same time enough copper stabilizer must be included in order to limit the Joule dissipation in case of quench. For these reasons, together with the very high stored energy, quench protection is one of the most challenging aspects of the design. In this paper, the quench protection of the cosθ design is presented. A standard quench protection study is accompanied by a less conservative study which includes AC effects on the power dissipation inside the coils and on the magnet inductance, in order to not exclude preventively more convenient designs, and to develop a more performing magnet as possible.**

***Index Terms* — Niobium compounds, quench protection, superconducting accelerators.**

## I. Introduction

THE Large Hadron Collider (LHC) at CERN has produced proton-proton collisions up to 8 TeV centre-of-mass energy in the period 2010-2013, and it reached 14 TeV in 2015-2016. After 2021, a luminosity upgrade is foreseen, named High Luminosity LHC (HL-LHC), after that the machine will be turned off. Then, new, more energetic particle accelerators will be needed in order to explore unknown regions of the high-energy physics. In this scenario, the project Future Circular Collider (FCC) [1] has started at CERN. Its goal is to develop three machines in a 100 km tunnel under the CERN site: an electron-electron collider (FCC-ee), an electron-proton collider (FCC-he) and a proton-proton collider (FCC-hh). In particular, the last one would be a machine able to produce proton collisions with 100 TeV centre-of-mass energy. In order to reach this target in a 100 km machine, the development of 16 T bending dipoles is needed.

The EuroCirCol [2] collaboration has started in 2015. It is part of the FCC project, under the European Community leadership, and it aims to develop a conceptual design of the machine within 2019. One of the goals is to develop a superconducting 16 T bending dipole [3]. The material chosen for the development is $Nb_3Sn$, because NbTi (which is the most used material for accelerator magnets) is limited to smaller magnetic fields. First $Nb_3Sn$ accelerator magnets will be inserted in the HiLumi-LHC, producing 10-12 T magnetic field, therefore the design and development of the FCC bending dipoles is one of the most challenging aspects. Three magnetic layouts have been explored by the EuroCirCol collaboration: a common-coil design [4], a block-coil design [5], and a cosθ design [6-7].

In this paper, the quench protection of the cosθ option is discussed and studied in deep. A first protection study has been already performed within the EuroCirCol collaboration [8-9], aiming to compare the three layouts with simple assumptions. Instead, in this paper, a more complete study is presented, focusing on the cosθ layout: a first protection scheme based on quench heaters is presented; the computation of the hot spot temperature is performed using nominal parameters, and it is accompanied also by a parametric study; moreover, this protection study is done using new electromagnetic models, developed for the HiLumi-LHC low-β quadrupoles protection, which take into consideration the AC dynamic effects on the magnet inductance [10-11].

## II. The Cosθ Layout

In Fig. 1, the cross section of the cosθ layout is showed. Table I reports the main parameters of the magnet, Table II reports the conductor features. It can be seen that the magnet is composed of four layers, assembled as two classic double-pancakes. Two conductors are used, one for layer 1 and 2 (HF conductor), one for layer 3 and 4 (LF conductor), supplied together with the same current. More details on the electro-magnetic and mechanical design can be found in [7].

In Fig. 2, the MIITs-T curve (at operating current) of the two conductors is represented, following the adiabatic approximation:

V. Marinozzi, G. Bellomo, M. Sorbi and G. Volpini are with University of Milano and INFN-LASA, Milan, Italy, email: vittorio.marinozzi@mi,infn,it.

T. Salmi and A. Stenvall are with Tampere University of Technology, Tampere, Finland, email: tiina.salmi@tut.fi.

B. Caiffi, P. Fabbricatore and S. Farinon are with INFN-Genova, Italy, email: stefania.farinon@ge.infn.it.

This work was supported by the European Union's Horizon 2020 research and innovation programme under grant No 654305, EuroCirCol project.

$$MIITs(T) = \frac{1}{A^2}\int_{T_0}^{T} \frac{\gamma(T)C_p(T)}{\varrho(B,RRR,T)}dT \qquad (1)$$

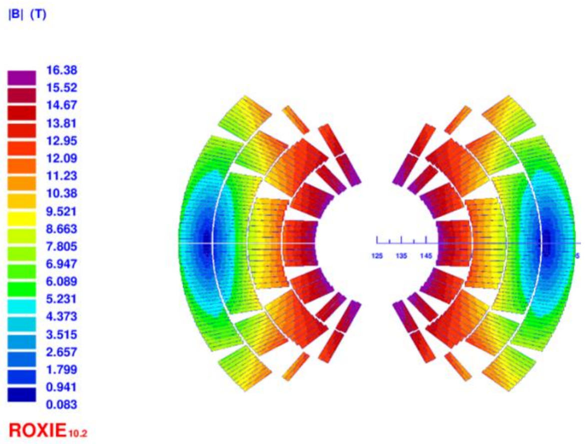


Fig. 1. Cross section of the 16T cosθ option and field map.

TABLE I MAIN PARAMETERS OF 16T COSΘ

| | |
|---|---|
| Bore diameter | 50 mm |
| Bore Magnetic field | 16 T |
| Length | 14.3 m |
| Operating current | 11180 A |
| Conductor peak field | 16.3 T |
| Operating temperature | 1.9 K |
| Inductance @$I_{op}$ | 19.9 mH/m |
| Stored magnetic energy | 1.3 MJ/m |
| Number of turns | 202 / aperture |

TABLE II CONDUCTOR FEATURES

| | HF conductor | LF conductor |
|---|---|---|
| Strand diameter | 1.1 mm | 0.712 mm |
| Strand number | 22 | 36 |
| Bare width | 13.2 mm | 13.5 mm |
| Bare thin/thick edge thickness | 1.892/2.072 mm | 1.225/1.343 mm |
| Insulation thickness | 0.15 mm | 0.15 mm |
| Keystone angle | 0.5° | 0.5° |
| Cu/NCu | 0.85 | 2.15 |
| Copper RRR | ≥100 | ≥100 |
| Operating point on load-line | 86 % | 86 % |

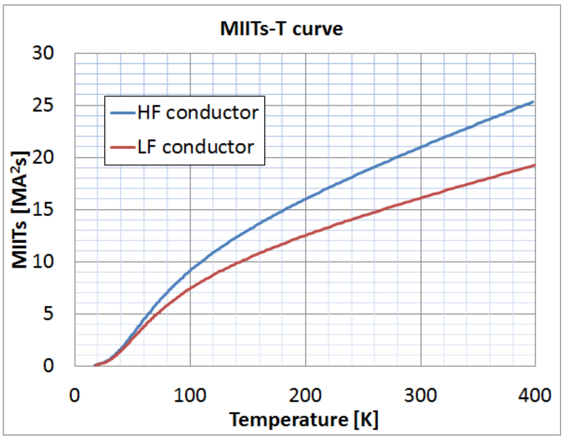


Fig. 2. MIITs-T curve at operating current of the HF and LF conductor.

where $T_0$ is the operating temperature, $A$ is the conductor area, $\gamma$ is the mass density, $C_p$ is the specific heat, and $\varrho$ is the electrical resistivity. The material properties used for the computation are from the MATPRO database [12]. As it could be expected, the most critical conductor is the LF one, therefore the protection study presented here will focus on it.

## III. PROTECTION HEATERS DESIGN

The quench protection heaters were designed considering the present state-of-the-art trace-based heater technology, which is used also in the HL-LHC inner triplet quadrupoles [11-13]. The heater strips are 25 µm thick stainless steel strips glued on a 75 µm thick layer of polyimide. The insulation thickness is increased by 50% from the HL-LHC quadrupole to account for the higher voltages.

### *A. Heater layout*

It is assumed that the two double-pancakes in cosθ are reacted separately, allowing placing of heaters on the surface of each coil layer. Based on simulations it was necessary to cover a large fraction of the coil surface to provoke a sufficiently wide normal zone in the coil. Fig. 3 shows the approximate locations of the heater strips, that cover 70% of the coil turns.

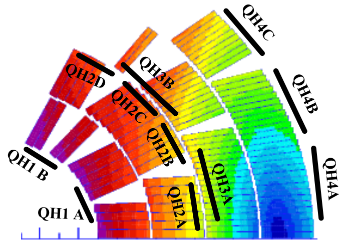


Fig. 3: Location of heater strips on coil surfaces.

Each heater strip is 14.3-m-long, and is based on heating stations. The heating station length is 5 cm in each strip and 25 cm long copper plated segment serves as a low-resistance bridge between them (see Fig. 4). The strips however have different widths as detailed in Table 3.

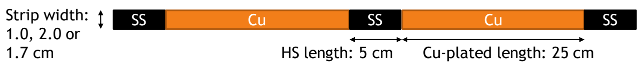


Fig. 4: A heater strip geometry: Each strip has 5 cm long stainless steel heating stations placed with 30 cm period. Three different strip widths are used: 1.0, 1.7 and 2.0 cm.

### *B. Heater powering*

For powering the heater strips in each half-coil are connected into three circuits. The circuits have 2,3 or 6 identical strips connected in parallel to a Heater Firing Unit (HFU) with charging voltage of 450 V and capacitance of 19.2 mF. In series with each heater strip parallel-connection is assumed 0.5 Ω resistance for wires. The resulting peak powers are in the range of 60-90 W/cm, and the circuit RC-time constants about 30 ms.

TABLE III
POWERING OF THE HEATER STRIPS IN ONE COIL-HALF WITH 3 HFU'S

| Circuit | QH strips | Strip width (cm) | $P_{QH}(0)$ (W/cm$^2$) | $\tau_{RC}$ (ms) |
|---|---|---|---|---|
| HFU#1 | 1A ‖ 1B ‖ 2A ‖ 2B ‖ 2C ‖ 2D | 1.0 | 67 | 25 |
| HFU#2 | 3B ‖ 4C ‖ 4B | 1.7 | 76 | 27 |
| HFU#6 | 3A ‖4A | 2.0 | 89 | 32 |

### *C. Simulated heater delays*

The heater delays were simulated using the 2-D heat diffusion model CohDA [14]. Fig.5 shows the delays as a function of magnetic field at 105% of operation current for the different considered heater powers and cables.

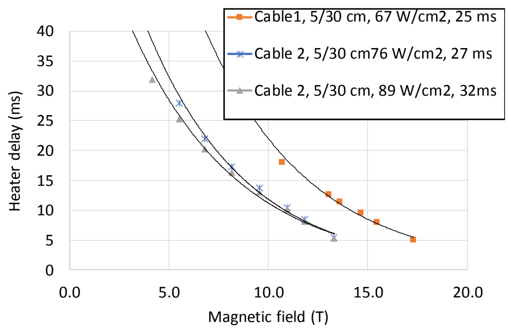


Fig. 5: Heater delays in cosθ simulated with CoHDA, at 105% of operation current.

## IV. Nominal Protection Study

The main goal of this protection study is to maintain the hot spot temperature (the temperature of the zone where the quench begins) within a certain level of safety. In this paper, the maximum allowed temperature will be considered as **350 K**. This number comes from the HiLumi-LHC experience with $Nb_3Sn$ [15].

The quench protection system presented here is based on the quench heaters discussed in section III. Table IV shows the other parameters used for the computation.

TABLE IV Protection Parameters

| | |
|---|---|
| Voltage threshold | 100 mV |
| Validation time | 10 ms |
| Switch opening delay time after validation | 1 ms |
| Inter-filament coupling currents average decay time | 15 ms |

Presence of dump resistor is not foreseen: as it can be seen in Table I, this magnet has large inductance and large stored energy, therefore the amount of energy that could be extracted in an external resistance would be negligible, just adding a complication for the voltage study.

The analysis has been performed using QLASA [16], making the following assumptions:

- The quench begins in the high field zone of the layer 3 (pole turn).
- The hot spot temperature is computed with adiabatic assumptions, following the computation showed in Fig. 2.
- Material properties are from MATPRO [12]
- The protection heaters delay time has been computed using CoHDA [14], following the scheme showed in Section III. Average values are used for the high-field and low-field zones of each layer.
- The quench is induced by heaters only in the turns covered by them; then, transversal propagation is taken into account.
- The quench is induced by heaters only under heating stations; then, longitudinal propagation is taken into account, while pre-heating coming from the heater copper sections is neglected.
- The differential inductance of the magnet is computed considering the dynamic effects of inter-filament coupling currents on it; details on the model implemented in QLASA can be found in [10] and [17].
- Inter-layer quench propagation is neglected.
- Quench back is neglected.
- Computation is performed at 105 % of the operating current.

The experimental validation of QLASA using similar assumptions can be found in [11].

Table V shows the resulting hot spot temperature and MIITs, comparing the nominal scenario with a computation done neglecting the AC dynamic effects on the inductance.

TABLE V Hot Spot Temperature

| Nominal | No dynamic effects | Coodi (No dyn eff) |
|---|---|---|
| 17.3 $MA^2s$ | 18.2 $MA^2s$ | 18.8 $MA^2s$ |
| 332 K | 357 K | 347 K |

It is easy to note that, according to the nominal scenario, the magnet can be considered protected, also with a margin of about 20 K on the maximum allowed temperature of 350 K. It is interesting to consider, too, that neglecting the effect of coupling currents on the magnet inductance, the protection of this magnet would be considered very hard to achieve, because the temperature rises of about 25 K, and it goes slightly over the maximum allowed.

The last column refers to another simulation performed with another quench simulation software, named Coodi [18]. This code uses constant propagation velocities (set at 20 m/s for the longitudinal propagation, at 10 cm/s for the transversal propagation), and material properties from the NIST database [19]; dynamic effects on the inductance are not included. It can be seen that, despite the larger amount of MIITs produced during the decay respect to the other cases, the hot spot temperature is lower, and within the limit of 350 K. This result shows that the choice of material properties strongly affects the protection study.

At this stage of the design, the analysis of heater failure scenarios has not been yet performed. It will be needed in future studies in order to ensure the protection redundancy.

## V. Parametric Study

In this section, a parametric study is presented, varying between reasonable values the most relevant parameters of the protection system and of the conductors. This study aims to show the direction to take for the future electromagnetic design upgrades of this magnet, in order to take the quench protection under control, or even to improve it, and to see how to eventually improve the protection parameters. The assumptions made are the same discussed in Section IV.

### A. *Voltage threshold and validation time dependence*

While the quench develops and the consequent resistance rises up, a growing with time resistive voltage appears between the ends of the magnet. This voltage can be therefore measured and used in order to detect a quench. The voltage threshold is the value beyond whom a quench is considered detected. However, superconductivity has for its own nature instabilities which cause voltage peaks; for this reason, after a quench is detected, it needs to be validated: the voltage has to stay over the threshold for a

certain time, called validation time. Only after that, the quench protection system is activated. Therefore, the choice of the voltage threshold and of the validation time has to be done with care: these two parameters have to be low enough in order to reduce the MIITs developed during detection and validation, but high enough in order to avoid false quench triggering due to superconductor instabilities.
In Fig. 6-left, the dependence of the temperature on the voltage threshold is showed, while in Fig. 6-right the dependence on the validation time is represented. The other parameters have been taken as the nominal ones.

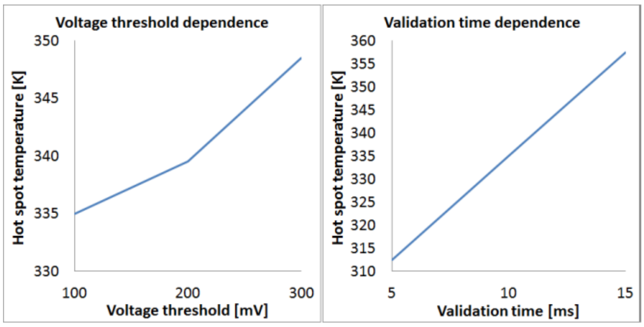

Fig. 6. Hot spot temperature dependence on the voltage threshold (left) and on the validation time (right)

It can be seen that the temperature does not strongly depends on the threshold, while the validation time has to be chosen with care, because every millisecond costs about 5 K.

### *B. Copper RRR dependence*

The RRR is defined as the ratio between the resistivity at room temperature and the resistivity at 10 K. A high RRR means that the copper is pure, and that its resistance at cold is low. Typically, a large RRR in the initial quench zone helps to maintain the hot spot temperature. Fig. 7 shows the dependence of hot spot temperature on the RRR of HF and LF conductor respectively.

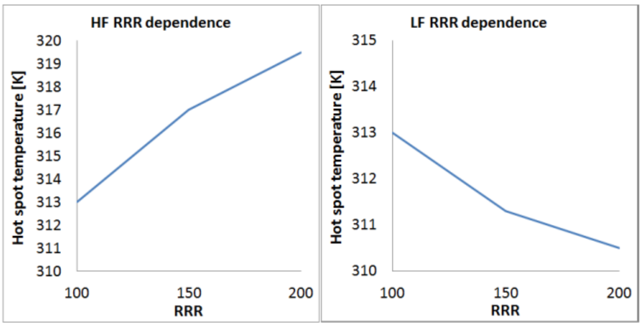

Fig. 7. Hot spot temperature dependence on the HF (left) and LF (right)conductor RRR.

It can be noted that the higher is the LF conductor RRR, the lower is the hot spot temperature, such as just explained. Nevertheless, for the HF conductor the behavior is opposite: this is due to the fact that the resistance developed by quench heaters is less with larger RRR. By the way, the dependence on RRR is light in both the cases.

### *C. Cu/NCu dependence*

The Cu/NCu is the ratio between the copper and the other material fractions within the strand. A large content of copper is usually preferable for the protection, because it reduces the copper current density and the heat dissipation; however, it decreases the margin on the load-line. Fig. 8 shows the hot spot temperature dependence on the Cu/NCu of HF and LF conductor respectively.

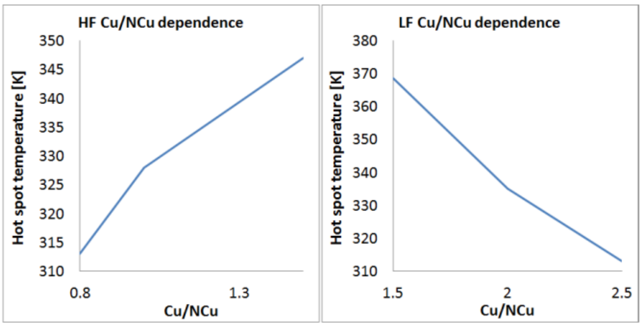

Fig. 8. Hot spot temperature dependence on the HF (left) and LF (right) conductor Cu/NCu

Also in this case, the behaviours are opposite: for the HF conductor, a larger amount of copper means that the resistance induced by heaters is lower, and that the hot spot temperature is therefore larger; instead, for the LF conductor, a larger amount of copper means that the initial quench zone warms slower, therefore the hot spot temperature decreases. By the way, the amount of copper have to be chosen with care, and with a good tolerance: in fact, every 0.1 costs 5-10 K in terms of hot spot temperature.

## VI. CONCLUSIONS

In this paper, the quench protection study of the Eurocircol cosθ dipole for FCC is presented. The protection is based on quench heaters, which have been designed with realistic assumptions. The nominal protection computation has been performed, showing that the hot spot temperature of the magnet can be maintained under control, within the safe value of 350 K. In particular, the use of novel electromagnetic models which simulate the effect of inter-filament coupling currents on magnet inductance helps to design more performing magnets.
Moreover, a parametric study has been performed, showing the dependence of the hot spot temperature on the main protection and conductor parameters. This work shows that the temperature depends in particular on the Cu/NCu of the two conductors and on the validation time, while it is slightly dependent on the RRR and on the voltage threshold. This study can be useful for future upgrades of the electro-magnetic design and for the development of the protection system.
In future studies, the analysis of failure scenarios will be carried on, in order to ensure the protection redundancy, and the analysis of peak voltages during a quench will be performed.

## REFERENCES


[1] https://fcc.web.cern.ch/Pages/default.aspx

[2] https://fcc.web.cern.ch/eurocircol/Pages/default.aspx

[3] D. Tommasini, et al., "The 16 T dipole development program for FCC", *IEEE Transactions on Applied Superconductivity*, presented at this conference.

[4] F. Toral, J. Munilla, T. Martinez , L. Garcia-Tabares, "The EuroCirCol 16T common-coil dipole option for the FCC ", *IEEE Transactions on Applied Superconductivity,* presented at this conference.

[5] C. Lorin, M. Durante, M. Segreti, EuroCirCol "16 T block-coils dipole option for the Future Circular Collider", *IEEE Transactions on Applied Superconductivity,* presented at this conference.

[6] V. Marinozzi, G. Bellomo, P. Fabbricatore, S. Farinon, M. Sorbi, G. Volpini, "Preliminary design of a superconducting main dipole for the future circular collider", *Physical Review Special Topic Accelerators and Beams*, submitted.

[7] M. Sorbi, G. Bellomo, B. Caiffi, P. Fabbricatore, S. Farinon, V. Marinozzi, G.Volpini, "The EuroCirCol 16T Cosine-Theta Dipole Option for the FCC", *IEEE Transactions on Applied Superconductivity*, presented at this conference.

[8] T. Salmi, A. Stenvall, M. Prioli, A. Ruuskenen, A. Verweij, B. Auchmann, D. Tommasini, D. Schoerling, C. Lorin, F. Toral, M. Durante, S. Farinon, V. Marinozzi, P. Fabbricatore, M. Sorbi, J. Munilla, "Quench protection analysis integrated in the design of 16 T Nb3Sn dipoles for the Future Circular Collider", *Physical Review Special Topic Accelerators and Beams*, submitted.

[9] T. Salmi, A. Stenvall, Marco Prioli, A. Verweij, B. Auchmann, V. Marinozzi, "Suitability of different quench protection methods for the 16 T Nb3Sn accelerator dipoles designed for the Future Circular Collider", *IEEE Transactions on Applied Superconductivity*, presented at this conference.

[10] V. Marinozzi, M. Sorbi, G. Manfreda, F. Bellina, H. Bajas and G. Chlachidze, "Effect of coupling currents on the dynamic inductance during fast transient in superconducting magnets", *Physical Review Special Topic Accelerators and Beams* 18, 032401, March 2015.

[11] V. Marinozzi, G. Ambrosio, G. Bellomo, G. Chlachidze, H. Felice, M. Marchevsky, T. Salmi, M. Sorbi, and E. Todesco, "Study of quench protection for the Nb3Sn low-β quadrupole for the LHC luminosity upgrade (HiLumi-LHC)", *IEEE Transactions on Applied Superconductivity*, vol. 25, no. 3, 2015.

[12] G. Manfreda, L. Rossi, and M. Sorbi, "MATPRO upgraded version 2012: a computer library of material property at cryogenic temperature," Tech. Rep. INFN-12-04/MI, INFN, April 2012.

[13] H. Felice et al., "Instrumentation and quench protection for LARP Nb3Sn magnets", IEEE Trans. Appl. Supercond., vol.19, no.3, pp. 2458-2462, Jun. 2009.

[14] T. Salmi, D. Arbelaez, S. Caspi, H. Felice, M. G. T. Mentink, S. Prestemon, A. Stenvall, and H. H. J. ten Kate, "A Novel Computer Code for Modeling Quench Protection Heaters in High-Field Nb3Sn Accelerator Magnets", *IEEE Transactions on Applied Superconductivity,* vol. 24, no. 4, 2014, Art. No. 4701810.

[15] E. Todesco, "Quench limits in the next generation of magnets" CERN Yellow Report 2013-006 10-16 (2013).

[16] L. Rossi and M. Sorbi, "QLASA: A computer code for quench simulation in adiabatic multicoil superconducting windings," Nat. Inst. of Nucl. Phys. (INFN), Rome, Italy, Tech. Rep. TC-04-13,2004.

[17] M. Sorbi, G. Ambrosio, H. Bajas, G. Chlachidze, V. Marinozzi, S. Mariotto, G. Sabbi, "Measurements and Analysis of Dynamic Effects in the LARP Model Quadrupole HQ02b during Rapid Discharge", *IEEE Transactions on Applied Superconductivity*, vol. 26, no. 4, 2016.

[18] T. Salmi and A. Stenvall, "The Impact of Protection Heater Delays Distribution on the Hotspot Temperature in a High-Field Accelerator Magnet", *IEEE Transactions on Applied Superconductivity*, vol. 26, no. 4, 2016.

[19] http://webbook.nist.gov/chemistry/